Electronic Supplementary Information

FeP embedded in N, P dual-doped porous carbon nanosheet: an efficient and durable bifunctional catalyst for oxygen reduction and evolution Reactions

Ruizhong Zhang, [1, 2] Chunmei Zhang, [1, 2] and Wei Chen*[1]

[1]*State Key Laboratory of Electroanalytical Chemistry, Changchun institute of Applied Chemistry, Chinese Academy of Sciences, Changchun 130022, Jilin, China, and*

[2]*University of Chinese Academy of Sciences, Beijing 100039, China*

E-mail: weichen@ciac.ac.cn

Experimental Details

1. Chemicals and materials.

Ferric chloride (FeCl$_3$·6H$_2$O, A.R., ≥99.0%, Tianjin East China Reagent Factory), phytic acid (C$_6$H$_{18}$O$_{24}$P$_6$, 70%, Xiya Reagent Research Center, Shandong, China), folic acid (C$_{19}$H$_{19}$N$_7$O$_6$, 98.0%, GEN-VIEW SCIENTIFIC INC.), potassium hydroxide (KOH, A.R., ≥85.0%, Beijing Chemical works), perfluorosulfonic acid-PTFE copolymer (Nafion, 5% w/w Solution, Alfa Aesar), E-TEK Pt/C (nominally 20% by wt. of 2-5 nm Pt nanoparticles on Vulcan XC-72R carbon support, Alfa Aesar). Nanopure water used in all experiments was supplied by a Water Purifier Nanopure water system (resistivity > 18 MΩ cm). All chemicals were commercially available and used without further purification.

2. Materials preparation.

2.1 Synthesis of iron phytate (FePA)

Iron phytate was synthesized from phytic acid and ferric chloride by a complexation-precipitation method. Typically, FeCl$_3$ (16.8 mL, 1.0 mol L^{-1}) and phytic acid (13.87 mL, 100 mg mL^{-1}) were mixed together in a round-bottomed flask. After vigorous stirring for 5 min, the solution color immediately changed to yellowish white. Then the flask was transferred into an oil bath with a pre-setting temperature of 100 °C to continue the complexation reaction for another 1 h. After cooled to room temperature, the resulting colloidal products were collected by centrifugation and washed several times with nanopure water. Finally, the obtained white products were dried in a conventional drying oven at 70 °C for 12 h and finely ground for further use.

2.2 Synthesis of FeP@NPCs hybrid nanomaterials

In a typical synthesis, iron phytate (FePA, 0.3 g) was first dispersed in 20 mL of nanopure water, followed by addition of 0.3 g folic acid for 30 min of stirring treatment. The obtained homogeneous mixture was sonicated for 1 h, further stirred for 8 h at room temperature. After that, the resulting precipitate was collected by centrifugation, and was dried in a conventional oven at 70 °C for 12 h.

The dried mixture was thoroughly ground into a homogeneous fine powder and then transferred into a ceramic boat. Next, the ceramic boat was placed at the center of a tubular furnace and the temperature was raised from 10 to 900 °C at a programming rate of 2.0 °C min^{-1} and then maintained at 900 °C for 2 h, and finally cooled to room temperature naturally. The whole heating process proceeds under N_2 atmosphere with a gas flow rate of 100 sccm. The carbonized products were leached with 0.5 M H_2SO_4 at 90 °C for 5 h to remove unstable species, excessive metals and metal oxides. The resulting products were separated by centrifugation, washed with an ethanol-ultrapure water mixture several times, and finally dried in a drying oven. For comparison, the nanocomposites without phytic acid or folic acid or iron salt or FePA were also prepared with the same procedure, which were denoted as Fe@NCs, Fe@PCs, NPCs and NCs, respectively.

3. Material characterization.

The morphologies of the samples were first studied by scanning electron microscope (FE-SEM, XL30 ESEMFEG) operating at 20 kV. The samples were prepared by drop-drying the ethanol suspension of catalysts onto ITO glass substrate. Transmission electron microscopy (TEM), high-resolution TEM (HRTEM) and the corresponding live fast Fourier transform (FFT), high-angle annular dark-field scanning transmission electron microscopy (HAAD-STEM), elements mapping and energy-dispersive X-ray (EDX) characterizations were all performed on a JEM-2010 (HR) microscope operated at 200 kV. The samples were prepared by drop-drying the ethanol suspension of samples onto carbon-coated copper grids. The surface chemical composition was determined by X-ray photoelectron spectroscopy (XPS, VG Thermo ESCALAB 250 spectrometer) operated at 120 W. The binding energies were calibrated against the carbon 1s line. Powder X-ray diffraction (XRD) patterns were collected using a D8 ADVANCE (Germany) Diffractometer using Cu Kα radiation with a Ni filter (λ = 0.154059 nm at 30 kV and 15 mA). The surface area and pore structure of the samples were characterized on an automatic gas adsorption/desorption analyzer (Quantachrome Instruments, version 3.01) with N_2 as adsorbate, and the samples were outgassed in vacuum at 200 °C for 24 h before test. The specific surface areas of the samples were calculated by the Brunauer-Emmett-Teller (BET) method using the adsorption

branch in the relative pressure range from 0.05-0.30. Raman spectra were collected on a Micro-Raman spectroscopy system RM 2000 (Renishaw in Via-reflex, 532 nm excitation laser).

4. Electrochemical measurements.

All electrochemical tests were carried out in a standard three-electrode cell at room temperature. A commercial rotating disk electrode (RDE) (AFE2M050GC, geometric area of 0.196 cm^2, Pine Research Instrumentation) covered by the catalyst with Nafion ionomer as a binder, a Pt coil and an Ag/AgCl (saturated KCl) electrode were used as the working electrode, counter electrode and reference electrode, respectively. The rotation rate and potential of the working electrode were controlled by a MSR Electrode Rotator (Pine Research Instrumentation) and a CHI 750 D electrochemical workstation. Before preparing the working electrode, 2 mg of catalyst was dispersed in 0.9 mL of ethanol and 0.1 mL of 5 wt % Nafion solution by sonication to form a 2 mg mL^{-1} homogeneous ink. Then the catalyst layer was prepared by dropping a calculated amount of catalyst ink onto a pre-polished RDE by a micropipettes and drying at room temperature. The loading of the catalysts was adjusted to be 0.2 mg cm^{-2}. The ORR activities of the catalysts were evaluated by RDE measurements in O$_2$-saturated 0.1 M KOH solution at a scan rate of 5 mV s^{-1}. Commercial Pt/C and RuO$_2$ were also measured for comparison, and the loading of Pt and RuO$_2$ catalysts on RDE was 24 μg$_{Pt}$ cm^{-2} and 81 μg cm^{-2}, respectively.

As for ORR, to obtain the electron transfer number (n), the RDE was scanned cathodically with varying speed from 225 to 2025 rpm in O$_2$-saturated 0.1 M KOH aqueous solution. The kinetic current density (J_K) can be calculated using the Koutecky-Levich equation which is expressed by

$$J_K = J_L J / J_L - J \qquad (1)$$

where J is the experimentally obtained current density, J_L refers to the measured diffusion-limited current density, and J_K is the mass-transport free kinetic current density.

The J_L term can be obtained from the Levich equation:

$$J_L = 0.2nFD^{2/3}\upsilon^{-1/6}\omega^{1/2}C_{O_2} \qquad (2)$$

where n is the number of electrons transferred; F is Faraday's constant (96 485 C mol^{-1}); D is the diffusion coefficient of O$_2$ in 0.1 M KOH solution (1.9 ×10^{-5} cm^2 s^{-1}); υ is the kinematic viscosity of the electrolyte (0.01 cm^2 s^{-1}); ω is the RDE rotation rate in rpm, and C_{O2} is the concentration of molecular oxygen in 0.1 M KOH solution (1.2×10^{-3} mol L^{-1}).

Rotating ring disk electrode (RRDE) measurements of the samples were tested on a glassy carbon disk (Φ 5.61 mm) with a polycrystalline Pt biased at 1.46 V (vs RHE) in 0.1 M KOH solution. The H$_2$O$_2$ yield (HO_2^- %) and the electrons transfer numbers (n) per oxygen molecule are calculated using the following equations:

$$n = \frac{4I_D}{I_D + I_R/N} \qquad (3)$$

$$HO_2^-\% = \frac{200\,I_R/N}{I_D + I_R/N} \qquad (4)$$

where I_R and I_D are ring and disk currents, and N is collection efficiency (0.37).

The accelerated durability tests (ADTs) of the catalysts were conducted by applying a cyclic potential sweep between 0.6 and 1.0 V (*vs* RHE) in O_2-saturated 0.1 M KOH solution at room temperature with a scan rate of 100 mV s^{-1}.

As for OER, linear sweep voltammograms (LSVs) tests were carried out using a catalyst-casted glassy carbon rotating disk electrode (RDE) prepared with the same procedure as ORR measurements and with the mass loading of 0.2 mg cm^{-2} in 0.1 M KOH with a scan rate of 5 mV s^{-1}. Prior to the measurements, the electrolyte (0.1 M KOH) was purged by O_2 for 15 min to maintain the O_2/H_2O equilibrium at 1.23 V (*vs* RHE) scale, and the working RDE was constantly rotating at 1600 rpm to remove the generated O_2 bubbles during the measurements. All polarization curves are corrected with 95% *iR*-compensation. The Tafel slopes are calculated according to the Tafel equation as follows:

$$\eta = b\log J + a \qquad (5)$$

where η is the overpotential, J is the current density, and b is the Tafel slope. The overpotential is calculated using the following equation:

$$\eta = E_{RHE} - 1.23 \qquad (6)$$

The electrochemically active surface areas (ECSA) of the as-prepared samples were roughly estimated from the electrochemical double-layer capacitance (C_{dl}) by measuring the non-Faradaic capacitive current associated with double-layer charging from the scan rate-dependent cyclic voltammograms in the potential range from 0.96 to 1.16 V (*vs* RHE). The scan rates of 5, 10, 20, 40, 60, 80 and 100 mV s^{-1} were used. The curves between ΔJ/2 at 1.06 V (*vs* RHE) and different scan rates were plotted. The C_{dl} was then estimated from the slope of the fitted curve in the linear region.

All the potentials referred to in this work are converted to the pH-dependent reversible hydrogen electrode (RHE): E (*vs* RHE) = E (*vs* Ag/AgCl) + 0.197 + 0.059 pH, and the current density is normalized to the geometric surface area of RDE or RRDE.
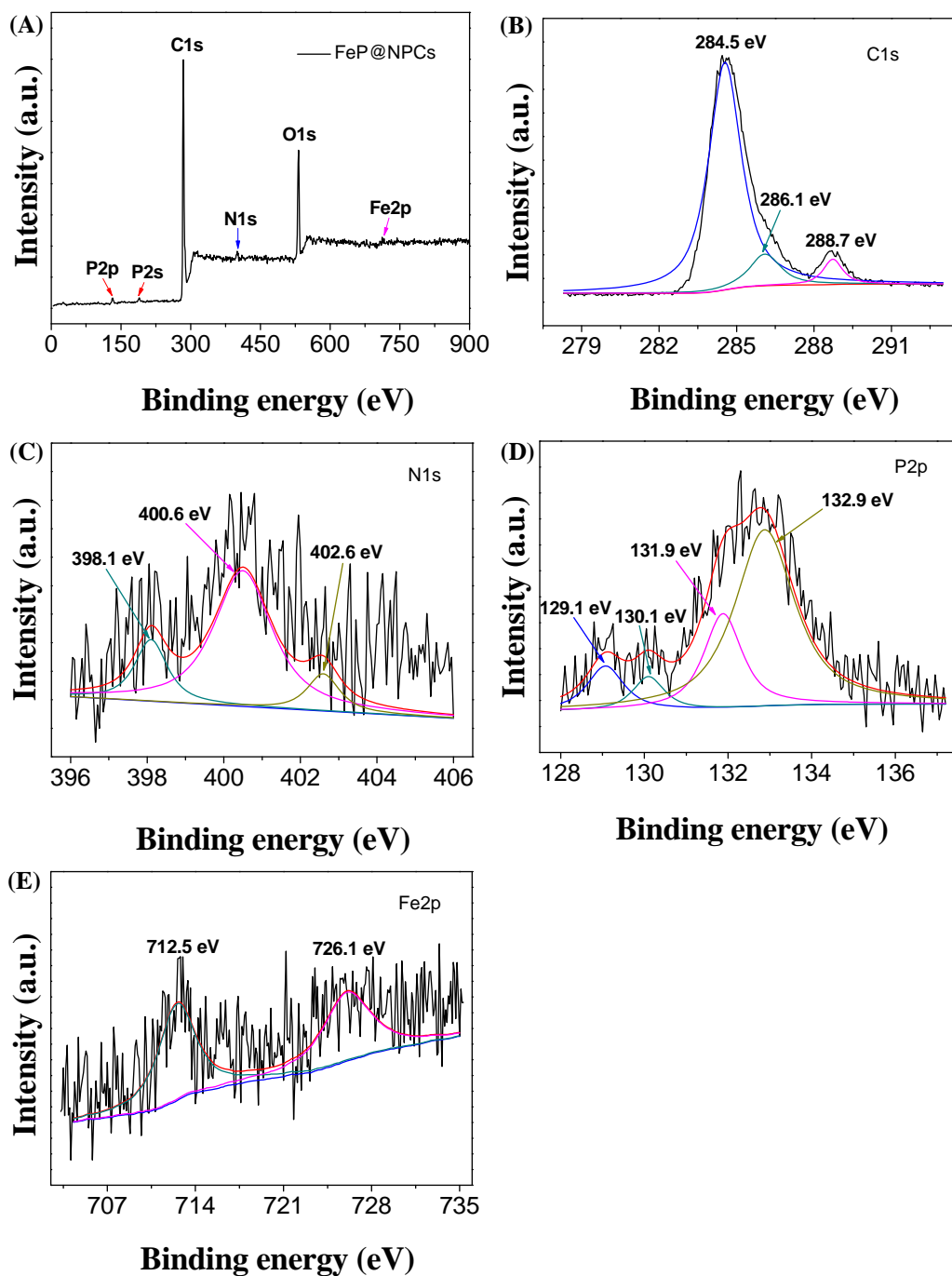
Supplementary Results

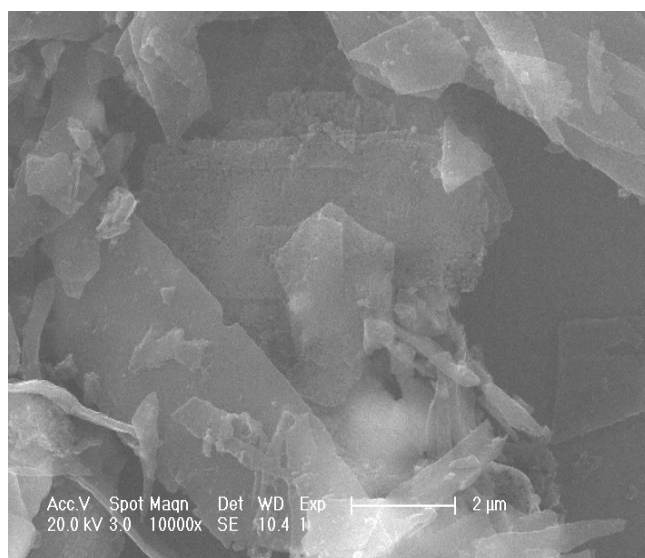| Element	At %
C	88.03
N	10.09
P	1.24
Fe	0.64
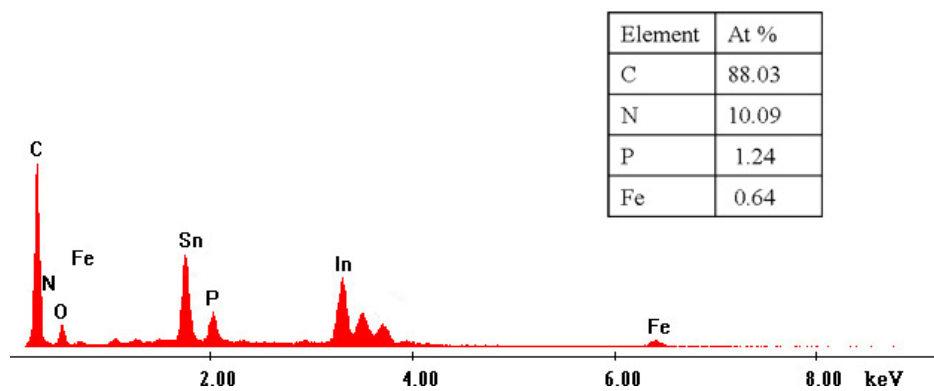
Fig. S1 Energy dispersive X-ray spectra (EDX) of FeP@NPCs. The signals of Sn and In come from the ITO glass substrate.
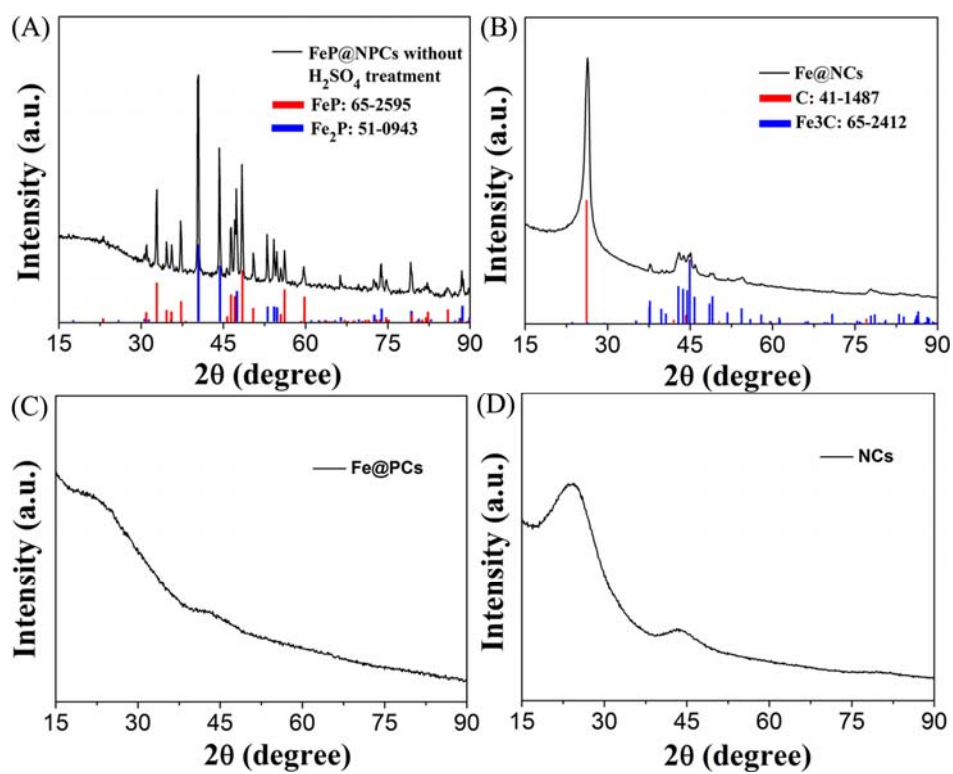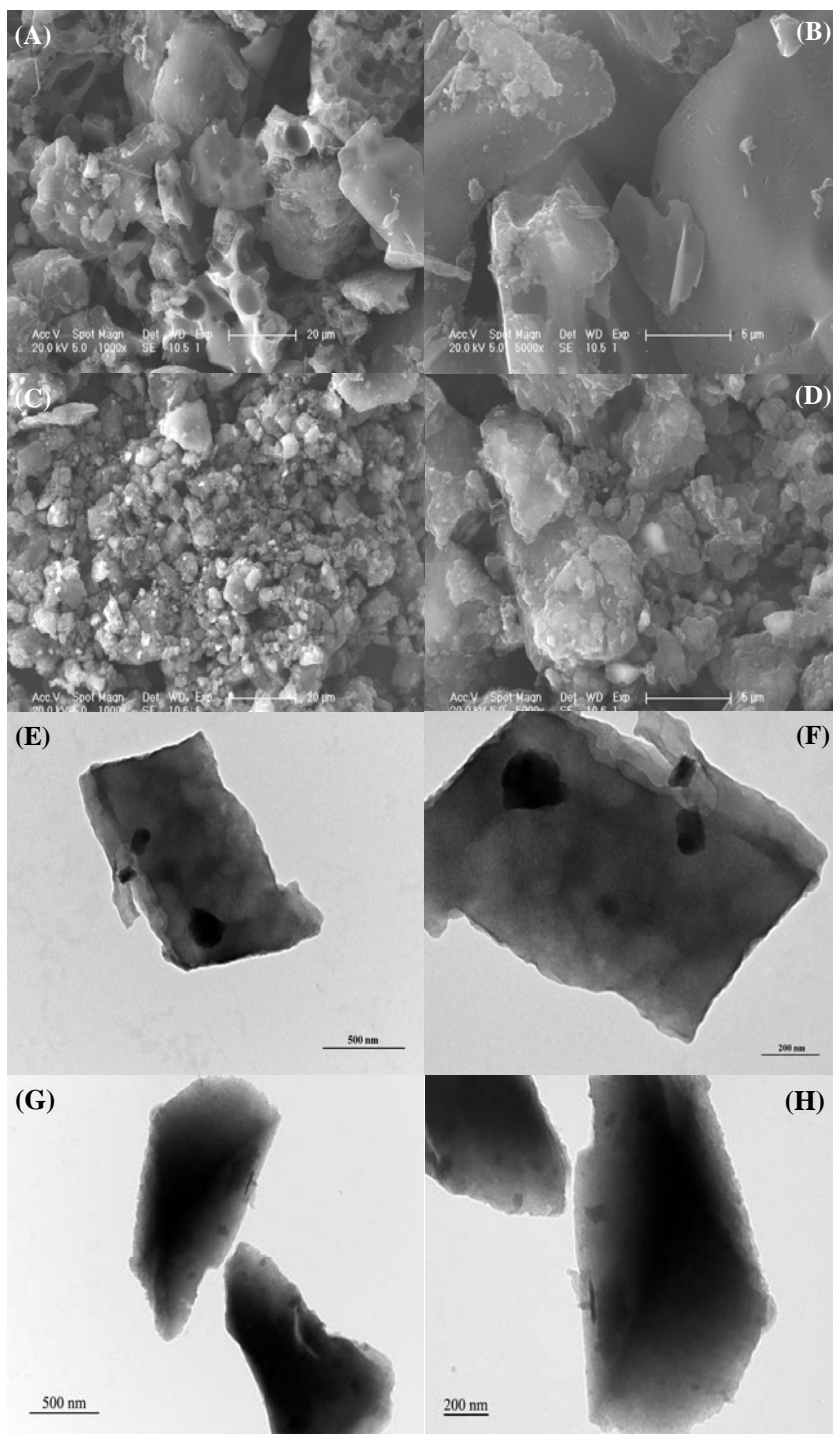
Fig. S2 XRD patterns of (A) FeP@NPCs without leached treatment by 0.5 M H_2SO_4, (B) Fe@NCs, (C) Fe@PCs and (D) NCs.
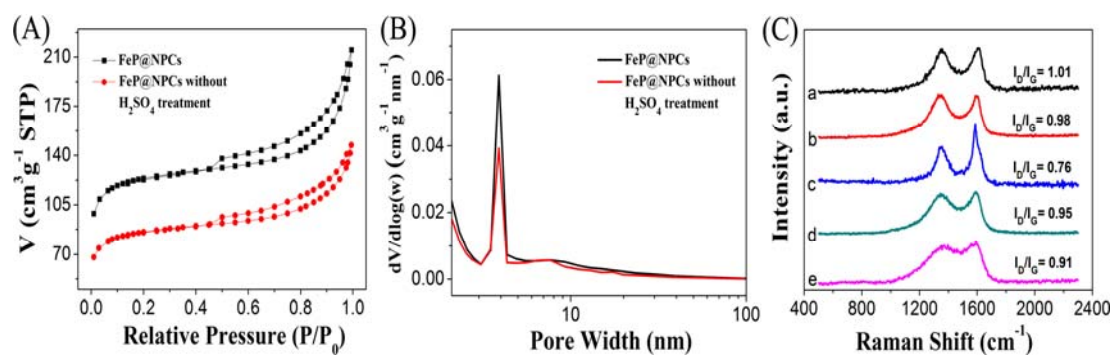
Fig. S3 XPS survey spectrum (A) and the corresponding high-resolution XPS spectra of C 1s (B), N 1s (C), P2p (D) and Fe 2p (E) of FeP@NPCs.

Fig. S4 A low-resolution SEM image of FeP@NPCs.

Fig. S5 SEM images of Fe@NCs (A, B) and Fe@PCs (C, D). TEM images of NCs (E, F) and NPCs (G, H).

Fig. S6 (A) Nitrogen adsorption/desorption isotherms and (B) the corresponding pore size distribution curves calculated from the desorption branches of FeP@NPCs with (black line) and without (red line) H_2SO_4 washing treatment. (C) Raman spectra of different samples: (a) FeP@NPCs, (b) FeP@NPCs without H_2SO_4 washing treatment, (c) Fe@NCs, (d) Fe@PCs and (e) NCs.
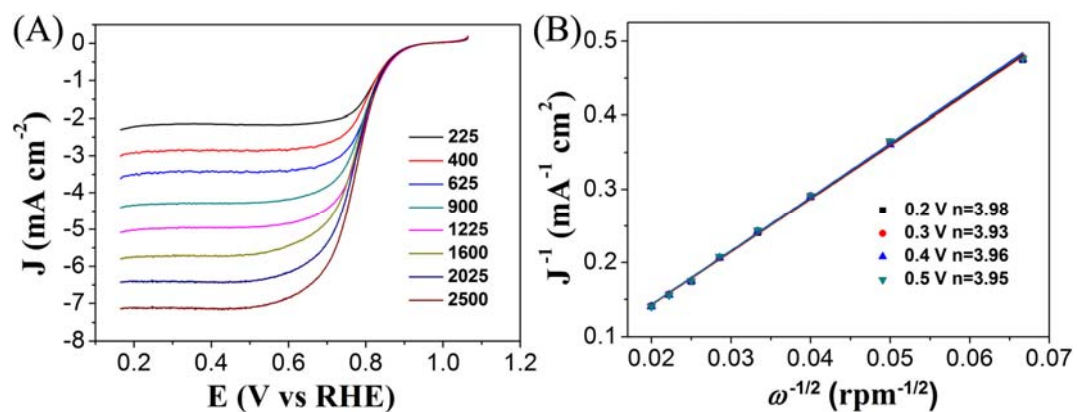
Fig. S7 ORR performance of the commercial Pt/C in alkaline medium: (A) Linear sweep voltammograms (LSVs) in O_2-saturated 0.1 M KOH at various rotation speeds with a scan rate of 5 mV s^{-1}, and (B) The corresponding K-L plots at different potentials.
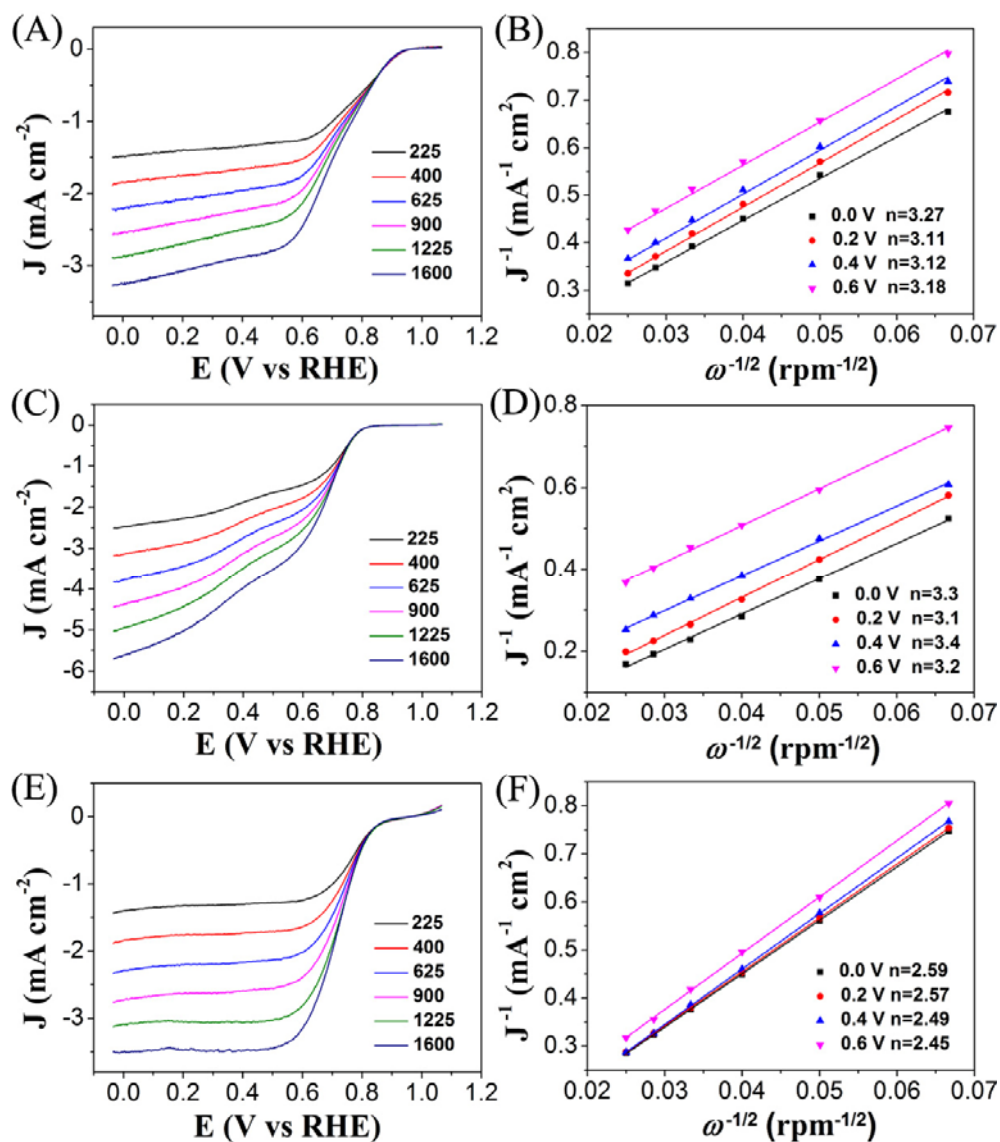
Fig. S8 Linear sweep voltammograms (LSVs) of ORR on (A) Fe@NCs, (C)Fe@PCs and (E) NCs in O$_2$-saturated 0.1 M KOH at various rotation speeds with a scan rate of 5 mV s^{-1}. The corresponding K-L plots at different potentials obtained from (B) Fe@NCs, (D) Fe@PCs and (F) NCs.
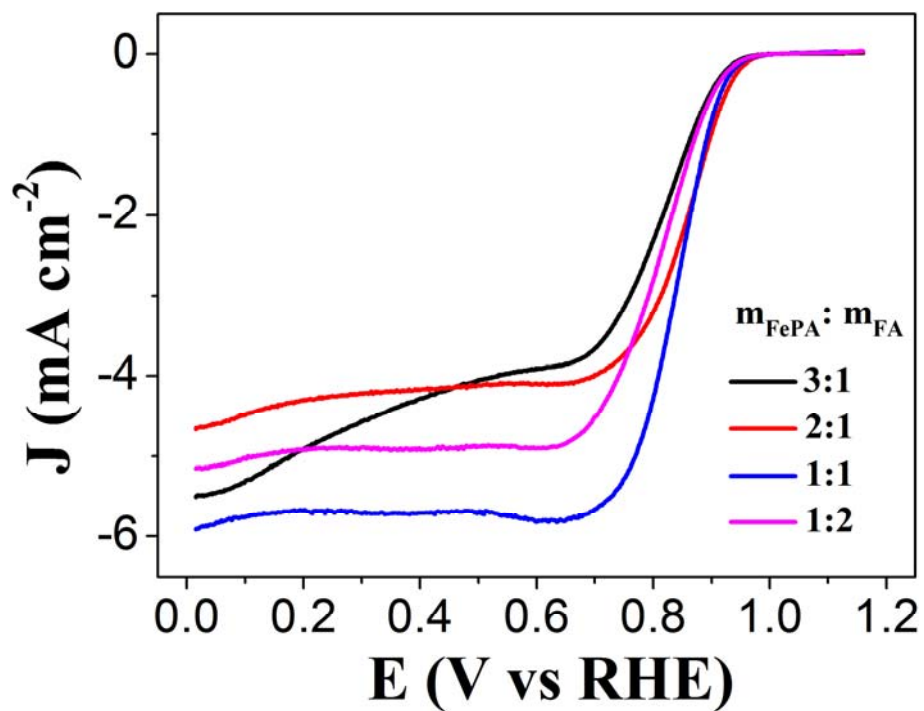
Fig. S9 RDE polarization curves of ORR on the FeP@NPCs catalyst pyrolyzed at 900 °C with different mass ratios of FePA and folic acid (FA) in O_2-saturated 0.1 M KOH solution with a scan rate of 5 mVs^{-1} at a rotation speed of 1600 rpm.
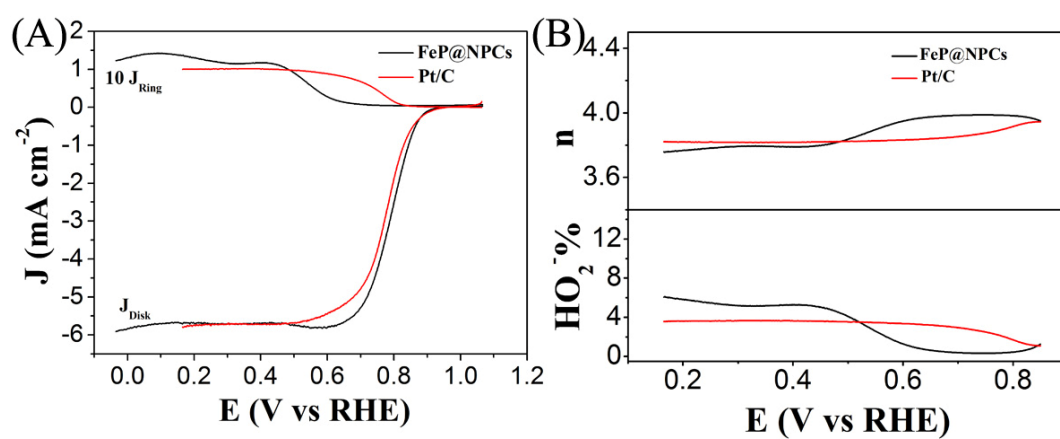
Fig. S10 (A) RRDE measurements of oxygen reduction (J_{Disk}) and hydrogen peroxide oxidation (J_{Ring}) on FeP@NPCs and commercial Pt/C in O_2-saturated 0.1 M KOH with a scan rate of 5 mV s^{-1} and rotation speed of 1600 rpm. (B) The corresponding H_2O_2 yield (HO_2^- %) and electron transfer number (*n*) on FeP@NPCs and commercial Pt/C.

.
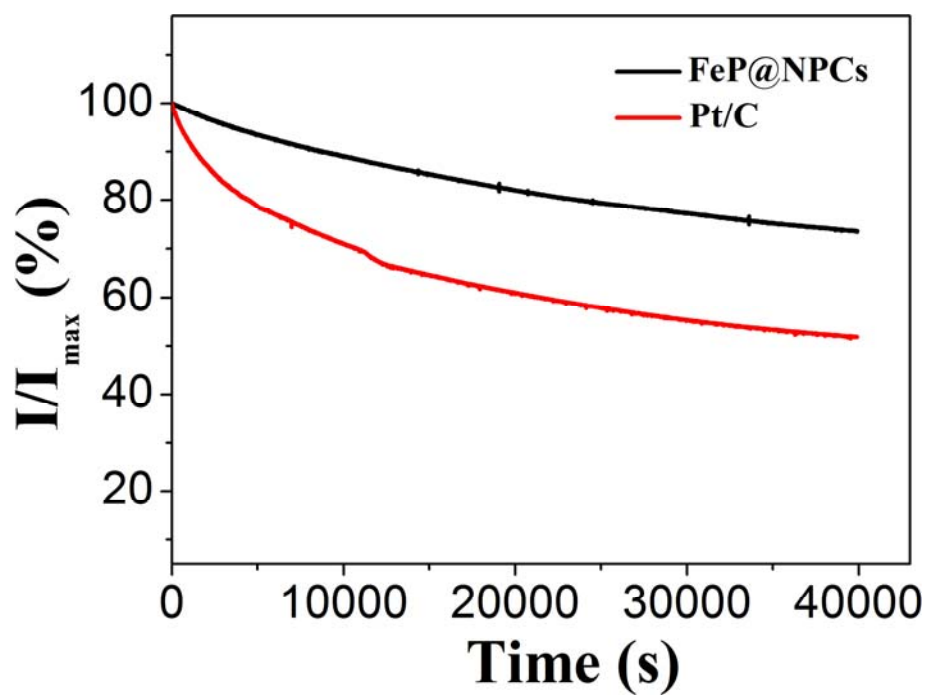
Fig. S11 Chronoamperometric measurements for FeP@NPCs and Pt/C catalysts in O_2-saturated 0.1 M KOH with the potential holding at 0.8 V (vs RHE) at a rotation rate of 900 rpm.
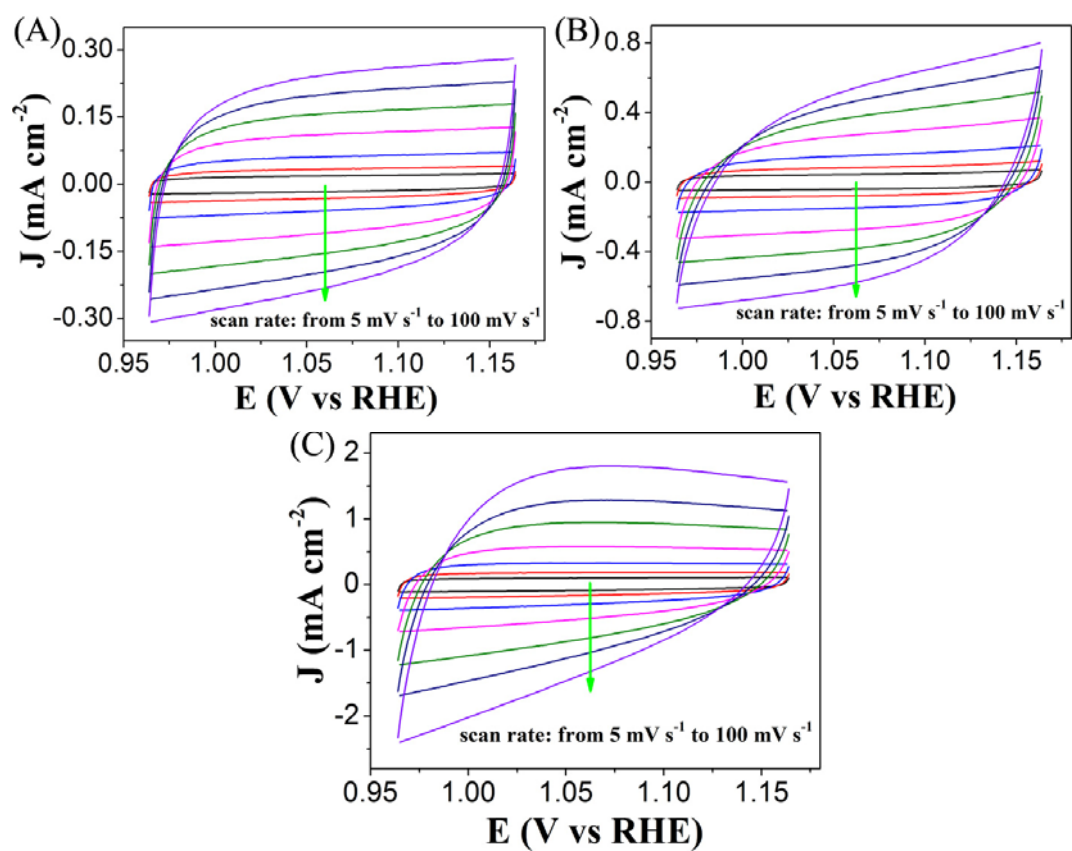
Fig. S12 Cyclic voltammograms curves of (A) Fe@NCs, (B) Fe@PCs and (C) NCs in a non-Faradaic region at different scan rates from 5 to 100 mV s^{-1}.
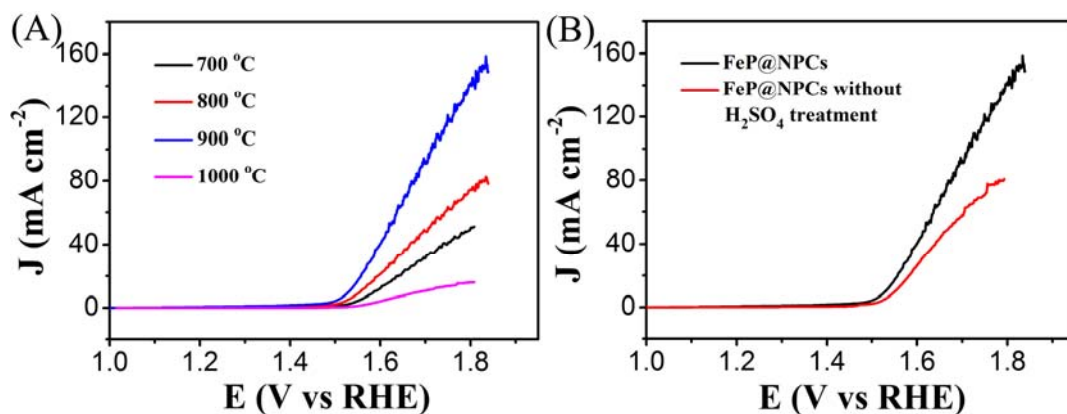
Fig. S13 (A) Comparison of OER catalytic activities of FeP@NPCs prepared at different temperatures. The used mass ratios of FePA/FA precursors are all of 1. (B) Comparison of OER catalytic activities of FeP@NPCs with and without H_2SO_4 leaching treatment. The annealing temperature is 900 °C and the mass ratio of FePA/FA is 1 for both samples. All of the LSV tests are performed at a rotation rate of 1600 rpm in 0.1 M KOH solution.
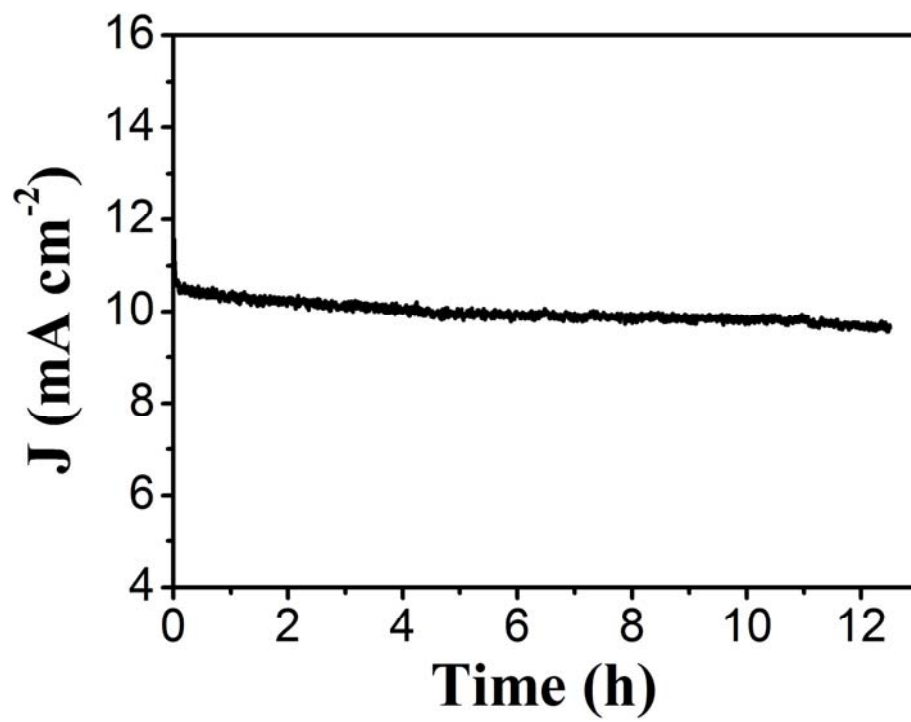
Fig. S14 Time-dependent current density of FeP@NPCs at an overpotential of 0.3 V for 12 h.

Table S1. Comparison of the bifunctional catalytic activities of FeP@NPCs with other reported electrocatalysts

Electrocatalyst	$E_{onset, ORR}$ (V)	$E_{onset, OER}$ (V)	$E_{1/2,ORR}$ (V) (-3 mA cm^{-2})	E_{OER} (V) (10 mA cm^{-2})	$\triangle E$ (V) (E_{OER}-E_{ORR})	Ref.
FeNi-LDH@3DG/CNTs	0.83	—	0.71	1.61	0.90	[1]
N-Co$_9$S$_8$/G	0.94	1.51	—	1.64	—	[2]
PCN-CFP	0.94	1.53	0.67	1.63	0.96	[3]
CNT@NCNT	0.99	—	0.63	1.76	1.33	[4]
N, P-GCNS	1.01	1.32	0.86	1.57	0.71	[5]
N-graphene/CNT	0.88	—	0.69	1.65	0.96	[6]
Co/N-C-800	0.83	—	0.74	1.60	0.86	[7]
CCH/C-2/C	0.93	—	0.82	1.74	0.92	[8]
Mn oxide	—	—	0.73	1.77	1.04	[9]
NiCo$_2$O$_4$-G	0.89	1.56	0.74	1.69	0.95	[10]
NoCo2S4@N/S-rGO	0.85	1.58	0.72	1.70	0.98	[11]
Co$_3$O$_4$/N-rmGO	0.88	—	0.85	1.54	0.69	[12]
FeP@NPCs	0.94	1.47	0.79	1.53	0.74	This work

References

1. Li, Y.; Zhao, M. J.; Zhao, Y.; Song, L.; Zhang, Z. P., FeNi Layered Double-Hydroxide Nanosheets on a 3D Carbon Network as an Efficient Electrocatalyst for the Oxygen Evolution Reaction. *Part. Part. Syst. Char.,* 2016, 33, 158-166.

2. Dou, S.; Tao, L.; Huo, J.; Wang, S. Y.; Dai, L. M., Etched and doped Co$_9$S$_8$/graphene hybrid for oxygen electrocatalysis. *Energ. Environ. Sci.* 2016, 9, 1320-1326.

3. Ma, T. Y.; Ran, J. R.; Dai, S.; Jaroniec, M.; Qiao, S. Z., Phosphorus-Doped Graphitic Carbon Nitrides Grown In Situ on Carbon-Fiber Paper: Flexible and Reversible Oxygen Electrodes. *Angew. Chem. Int. Ed.* 2015, 54, 4646-4650.

4. Tian, G. L.; Zhang, Q.; Zhang, B. S.; Jin, Y. G.; Huang, J. Q.; Su, D. S.; Wei, F., Toward Full Exposure of "Active Sites": Nanocarbon Electrocatalyst with Surface Enriched Nitrogen for Superior Oxygen Reduction and Evolution Reactivity. *Adv. Funct. Mater.* 2014, 24, 5956-5961.

5. Li, R.; Wei, Z. D.; Gou, X. L., Nitrogen and Phosphorus Dual-Doped Graphene/Carbon Nanosheets as Bifunctional Electrocatalysts for Oxygen Reduction and Evolution. *ACS Catal.* 2015, 5, 4133-4142.

6. Wen, Z. H.; Ci, S. Q.; Hou, Y.; Chen, J. H., Facile One-Pot, One-Step Synthesis of a Carbon Nanoarchitecture for an Advanced Multifunctonal Electrocatalyst. *Angew. Chem. Int. Ed.* 2014, 53, 6496-6500.

7. Su, Y. H.; Zhu, Y. H.; Jiang, H. L.; Shen, J. H.; Yang, X. L.; Zou, W. J.; Chen, J. D.; Li, C. Z., Cobalt

nanoparticles embedded in N-doped carbon as an efficient bifunctional electrocatalyst for oxygen reduction and evolution reactions. *Nanoscale* 2014, 6, 15080-15089.

8. Wang, Y.; Ding, W.; Chen, S. G.; Nie, Y.; Xiong, K.; Wei, Z. D., Cobalt carbonate hydroxide/C: an efficient dual electrocatalyst for oxygen reduction/evolution reactions. *Chem. Commun.* 2014, 50, 15529-15532.

9. Gorlin, Y.; Jaramillo, T. F., A Bifunctional Nonprecious Metal Catalyst for Oxygen Reduction and Water Oxidation. *J. Am. Chem. Soc.* 2010, 132, 13612-13614.

10. Lee, D. U.; Kim, B. J.; Chen, Z. W., One-pot synthesis of a mesoporous $NiCo_2O_4$ nanoplatelet and graphene hybrid and its oxygen reduction and evolution activities as an efficient bi-functional electrocatalyst. *J. Mater. Chem. A* 2013, 1, 4754-4762.

11. Liu, Q.; Jin, J. T.; Zhang, J. Y., $NiCO_2S_4$@graphene as a Bifunctional Electrocatalyst for Oxygen Reduction and Evolution Reactions. *ACS Appl. Mat. Interfaces* 2013, 5, 5002-5008.

12. Liang, Y. Y.; Li, Y. G.; Wang, H. L.; Zhou, J. G.; Wang, J.; Regier, T.; Dai, H. J., Co_3O_4 nanocrystals on graphene as a synergistic catalyst for oxygen reduction reaction. *Nat. Mater.* 2011, 10, 780-786.